ELSEVIER

International Journal of Mass Spectrometry 185/186/187 (1999) 107–116

International Journal of Mass Spectrometry

Gas phase copper(I) ion affinities of valine, lysine, and arginine based on the dissociation of Cu^+-bound heterodimers at varying internal energies

Blas A. Cerda, Chrys Wesdemiotis*

Department of Chemistry, The University of Akron, Akron, OH 44325, USA

Received 11 May 1998; accepted 3 August 1998

Abstract

The Cu^+ affinities of the amino acids valine (Val), lysine (Lys), and arginine (Arg) are determined in the gas phase based on the dissociations of Cu^+-bound dimers $[A + B_i]Cu^+$, in which A represents one of the three amino acids studied and B_i a set of different amino acids of known Cu^+ affinity (kinetic method). In order to deconvolute entropic contributions from experimentally measured free energies, the decompositions of $[A + B_i]Cu^+$ are assessed as a function of internal energy using angle-resolved mass spectrometry. The Cu^+ affinities deduced for Val, Lys, and Arg are 283, 355, and 364 kJ mol^{-1}, respectively. Lysine and arginine are found to have substantially larger entropies of Cu^+ attachment when compared to valine. The combined affinity and entropy data are consistent with participation of the flexible side chain substituents of lysine and arginine in the coordination of Cu^+, yielding multidentate complexes of markedly higher stability than the aliphatic amino acid valine. (Int J Mass Spectrom 185/186/187 (1999) 107–116) © 1999 Elsevier Science B.V.

Keywords: Cu^+ affinity; Lysine; Arginine; Entropy effects; Angle-resolved mass spectrometry

1. Introduction

Copper ions are among the most conspicuous transition-metal ions in living systems. Numerous copper complexes of proteins exist and in several instances these complexes are essential for vital biochemical processes, such as dioxygen transport and electron transfer [1]. The amino acid composition and sequence of a copper ion binding protein are important variables in both the selection of the metal ion's attachment site as well as the resulting biological activity of the complex [1,2]. For example, copper-storing metallothioneins are cysteine-rich, while the copper-binding dioxygen transport enzymes carry a large number of histidine residues [1,2]. Understanding the principles governing the interaction of copper ions with amino acids and peptides, i.e. of protein constituents, has therefore been a subject of great interest in solution studies [1–3].

Regarding copper(I), the intrinsic chemistry of its adducts with amino acids and peptides has been devoted considerable interest by mass spectrometry and theory. Gross *et al*. showed that the fragmentations of $[GlyGlyLeu]Cu^+$ and $[GlyGlyLeu]Na^+$ differ, possibly due to distinct binding locations for Cu^+

* Corresponding author.

Dedicated to Professor Michael T. Bowers for his 60th birthday and his pioneering contributions to gas phase ion chemistry.

PII S1387-3806(98)14132-5

versus Na^+ [4]. Nelson and Hutchens found a correlation between the number of Cu^+ ions attached to oligopeptides and the number of histidine residues present in those peptides, suggesting histidine to be the most probable binding site [5]. Bouchonnet et al. [6], Wen et al. [7], Lei and Amster [8], Polce et al. [9], and Lavanant and Hoppilliard [10] analyzed, in detail, the unimolecular reactions of Cu^+-cationized amino acids, which were shown to yield both organometallic and organic products. The selection of the preferred Cu^+ binding site in a peptide or amino acid and the ensuing fragmentations of the Cu^+ adduct have been presumed to depend on the intrinsic Cu^+ affinities of the individual amino acid residues [4–8]. For more information on this issue, several research groups have examined, experimentally or computationally, the bond energies of Cu^+ to amino acids [11,12] and to relevant model systems [13–15]. A previous study from our laboratory [11], reported the relative Cu^+ affinities of 18 of the 20 common α-amino acids based on the dissociations of their Cu^+-bound heterodimers (Cooks' kinetic method [16,17]). The largest measurable Cu^+ affinity was found for histidine (56 kJ mol^{-1} above glycine [11]). A subsequent theoretical study by Hoyau and Ohanessian derived the absolute Cu^+ affinities of glycine, serine, and cysteine at high ab initio level [12]; the calculated affinity differences between Ser and Gly and between Cys and Gly were found to be in excellent agreement with the relative Cu^+ affinities reported by us [11], prompting the authors to combine their calculated "anchor" values with our experimental relative Cu^+ affinity scale to obtain the absolute Cu^+ affinities of all mammalian amino acids except lysine and arginine. For the latter two amino acids, our earlier study was unable to provide the values of their relative Cu^+ affinities because of entropic problems (vice infra). The present investigation closes this gap by determining the Cu^+ affinities of lysine and arginine using a modified version of the kinetic method in conjunction with angle-resolved mass spectrometry (ARMS) [18–20], an approach that can account for entropy effects [21–25].

2. Methods

The copper(I) ion affinity, $\Delta H^\circ_{Cu^+}$, of an amino acid (A) corresponds to the bond dissociation enthalpy of the A–Cu^+ bond, as defined by

$$[A]Cu^+ \rightarrow A + Cu^+, \qquad \Delta H^\circ_{rxn} = \Delta H^\circ_{Cu^+}. \quad (1)$$

Breakup of the A–Cu^+ bond also causes changes in entropy ($\Delta S^\circ_{Cu^+}$) and free energy ($\Delta G^\circ_{Cu^+}$), which are interrelated via

$$\Delta G^\circ_{Cu^+} = \Delta H^\circ_{Cu^+} - T\Delta S^\circ_{Cu^+}. \quad (2)$$

The Cooks kinetic method compares a molecule of unknown $\Delta G^\circ_{Cu^+}$ to one whose $\Delta G^\circ_{Cu^+}$ has been established [16,17]. This is accomplished by forming the Cu^+-bound dimer of the relevant molecules and assessing the dissociation kinetics of the dimer to the individual copper-attached monomers. For heterodimers between an amino acid (A) and a series of different amino acids (B_i) serving as the reference bases, viz. $[A + B_i]Cu^+$, the pertinent dissociations are given in

$$[A]Cu^+ + B_i \xleftarrow{k} [A + B_i]Cu^+ \xrightarrow{k_i} A + [B_i]Cu^+. \quad (3)$$

Based on the thermodynamic formulation of transition state theory [26], the natural logarithm of the rate constant ratio of the competing unimolecular reactions of Eq. (3) depends on the relative free energy of activation of these processes and the effective temperature of the decomposing dimer, as given by

$$\ln(k/k_i) = -\Delta(\Delta G^\ddagger)/RT_{eff} = -\Delta(\Delta H^\ddagger)/RT_{eff} + \Delta(\Delta S^\ddagger)/R. \quad (4)$$

The term $\Delta(\Delta G^\ddagger)$, which describes the difference in free energies of activation for breaking the A–Cu^+ versus the B_i–Cu^+ bond, contains contributions from the corresponding relative entropy and enthalpy of activation, as also shown in Eq. (4).

Cu^+ forms electrostatic bonds with organic ligands, which generally dissociate with no reverse activation energy [27]. Under these conditions, the

relative activation functions $\Delta(\Delta G^{\ddagger})$, $\Delta(\Delta S^{\ddagger})$, and $\Delta(\Delta H^{\ddagger})$ become numerically equal (with opposite sign) to the *relative* thermodynamic functions $\Delta(\Delta G^{\circ}_{Cu^+})$, $\Delta(\Delta S^{\circ}_{Cu^+})$, and $\Delta(\Delta H^{\circ}_{Cu^+})$, which are the differences in free energy, entropy, and affinity, respectively, between the A–Cu^+ and B_i–Cu^+ bonds; this equivalence leads to

$$\ln(k/k_i) = \Delta(\Delta G^{\circ}_{Cu^+})/RT_{eff} = \Delta(\Delta H^{\circ}_{Cu^+})/RT_{eff} - \Delta(\Delta S^{\circ}_{Cu^+})/R. \quad (5)$$

Eq. (5) indicates that the kinetic method probes free energies (often referred to as "basicities"), not enthalpies (affinities), unless the entropic parameter is negligible. $\Delta(\Delta S^{\circ}_{Cu^+}) \approx 0$ if the two ligands compared in the $[A + B_i]Cu^+$ dimer have similar entropies of Cu^+ attachment. This prerequisite has been found to be valid when A and B_i are any two common α-amino acids except lysine and arginine [11]. As a result, in dimers containing Lys or Arg (A) and one of the other eighteen amino acids as reference (B_i), $\Delta(\Delta S^{\circ}_{Cu^+}) = \Delta S^{\circ}_{Cu^+}(A) - \Delta S^{\circ}_{Cu^+}(B_i)$ cannot be neglected; nevertheless, this entropy difference remains approximately constant within a $[Lys + B_i]Cu^+$ or $[Arg + B_i]Cu^+$ series because of the similar entropies of Cu^+ attachment of the B_i members [11]. In such a case, Eq. (5) can be expanded to

$$\ln(k/k_i) = [\Delta H^{\circ}_{Cu^+}(A)/RT_{eff} - \Delta(\Delta S^{\circ}_{Cu^+})/R] - \Delta H^{\circ}_{Cu^+}(B_i)/RT_{eff}, \quad (6)$$

where the variables remaining constant within a $[A + B_i]Cu^+$ set have been combined in brackets. The quantity within brackets represents an apparent Cu^+ basicity of A, viz. $\Delta G^{app}_{Cu^+}(A)$, as defined by

$$\Delta G^{app}_{Cu^+}(A)/RT_{eff} = \Delta H^{\circ}_{Cu^+}(A)/RT_{eff} - \Delta(\Delta S^{\circ}_{Cu^+})/R. \quad (7)$$

The experiment measures the rate constant ratios k/k_i, which are equal to the ratios of the abundances of $[A]Cu^+$ and $[B_i]Cu^+$ in the appropriate tandem mass spectra of $[A + B_i]Cu^+$. A plot of $\ln(k/k_i)$ versus $\Delta H^{\circ}_{Cu^+}(B_i)$ leads to a regression line whose slope and intercept provide, based on Eqs. (6) and (7), T_{eff} and $\Delta G^{app}_{Cu^+}(A)$ at this T_{eff}, respectively. Repeating the experiment at several effective temperatures furnishes a set of T_{eff} and $\Delta G^{app}_{Cu^+}(A)$ values, from which a new plot of $\Delta G^{app}_{Cu^+}(A)/RT_{eff}$ against $1/RT_{eff}$ can be constructed. The resulting regression line affords, according to Eq. (7), $\Delta H^{\circ}_{Cu^+}(A)$ from its slope and $\Delta(\Delta S^{\circ}_{Cu^+})$ from its intercept. This modified version of the kinetic method has been successfully used by Fenselau and co-workers [21,22] and us [23–25] to deduce proton affinities and metal ion affinities of biomolecules for which dimers with $\Delta(\Delta S^{\circ}) \approx 0$ are unavailable.

Several different approaches can be applied to vary the effective temperature which represents a measure of the average internal energy of the dissociating dimer ions [28,29]. Using collisional activation with gaseous targets, T_{eff} can be varied by changing the laboratory frame kinetic energy (E_{lab}) or the target mass [30], as demonstrated by Fenselau and co-workers [21,22] and us [23–25], respectively. An alternative method involving angle-resolved mass spectrometry (ARMS) [18–20, 30] is examined here. ARMS allows one to change T_{eff} of kiloelectron volt ions gradually and in small steps, as does varying E_{lab} in the electron volt range; in contrast, variations of the collision target cause larger and less controllable alterations to T_{eff}. ARMS exploits the fact that the internal energy of a dimer ion which collides with a target gas is related to the angle through which the ion is inelastically scattered [18–20]. Approximate selection of ion internal energies (and, thus, ion effective temperatures) is possible by altering the scattering angle (θ) at which the products from collisionally activated dissociation are observed. In this investigation, the kinetic method/ARMS variant is applied to first replicate the reported Cu^+ affinity of valine [11,12] and then determine the Cu^+ affinities of lysine and arginine (Scheme 1).

3. Experimental

All experiments were performed with a modified VG AutoSpec tandem mass spectrometer of E_1BE_2 geometry, which is equipped with two collision cells

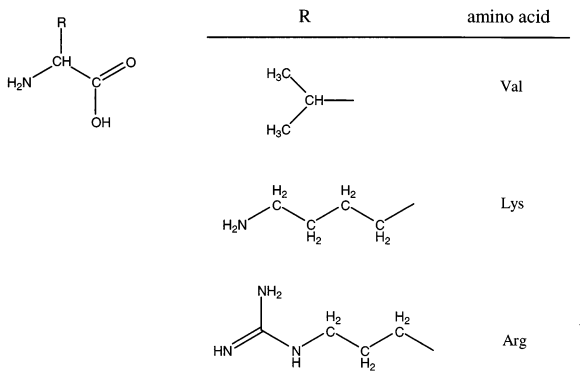

Scheme 1.

(CC-1 and CC-2) and an intermediate deflector electrode in the field-free region between E_1B (MS-1) and E_2 (MS-2) [31]. Methanol and n-butylbenzene were ionized by electron impact (EI) at 70 eV. The copper(I) ion-bound heterodimers $[A + B_i]Cu^+$ were generated by fast atom bombardment (FAB) using ~12 keV Cs^+ ions as bombarding particles and glycerol as the matrix. The molecular ions of methanol and n-butylbenzene or the $[A + B_i]Cu^+$ precursor ions were accelerated to 8 keV, mass selected by MS-1, and allowed to dissociate spontaneously or by collision in the field-free region between MS-1 and MS-2. The fragment ions thus produced were dispersed by MS-2 and recorded in the corresponding metastable ion (MI) or collisionally activated dissociation (CAD) mass spectrum, respectively. For CAD, helium was introduced in CC-2 until the precursor ion beam was attenuated by 20%. The MI and CAD spectra measured are multiscan summations and reproducible to better than ±5%. Kinetic energy releases of MI signals were calculated from peak widths at half height ($T_{0.5}$) by established procedures [32,33].

To obtain angle-resolved CAD mass spectra, the mass-selected precursor ion beam was deflected in the x–y plane prior to collision with He gas in CC-2, by applying a positive potential to the deflector electrode situated in front of CC-2. The relationship between deflector potential (U_c) and ion beam deflection angle (θ_{lab}) is given by [19]

$$\tan\theta = (l/2d)(U_c/U_b), \quad (8)$$

where d is the distance between the deflection plates, l is the length of the deflection plates, and U_b is the ion beam accelerating potential.

The copper-bound amino acid dimer samples were prepared from saturated solutions (in the matrix) of the appropriate amino acids and cupric acetate. To generate the desired heterodimer ion, ~0.5 mL aliquots of the individual stock solutions were mixed and a few microliters of the resulting mixture were transferred onto the FAB probe tip. This procedure maximized the intensity of $[A + B_i]Cu^+$. The abundance of the heterodimer ions in the FAB spectrum was approximately 1%–5% of the base peak (usually protonated matrix or protonated amino acid). All substances were purchased from Aldrich or Sigma and were used without any modification.

4. Results and discussion

Initially, the angle-resolving capabilities of our instrument are tested by acquiring angle-resolved CAD mass spectra for methanol and n-butylbenzene ions, from which the corresponding breakdown curves are constructed. These are then compared with reported ARMS breakdown data for methanol [19] and the reported photoelectron–photoion coincidence (PEPICO) breakdown graph of n-butylbenzene [34]. The performance of the combined kinetic method/ARMS procedure is subsequently examined by deriving the known Cu^+ affinity of valine [11,12], using as reference set (B_i) the amino acids alanine, serine, leucine and isoleucine. Finally, $\Delta H^\circ_{Cu^+}$ of lysine and arginine are measured following the same protocol, using as B_i set phenylalanine, tryptophan and histidine (for Lys) or glutamine and histidine (for Arg). With the reference bases selected, it was possible to form sufficiently abundant $[A + B_i]Cu^+$ dimers that produce *both* $[A]Cu^+$ *and* $[B_i]Cu^+$ with measurable intensities. The published copper(I) ion affinities of the reference amino acids are summarized in Table 1 [11,12]; these amino acids (and all other common α-amino acids except Lys and Arg) were shown to have similar entropies of Cu^+ complexation [11], as

Table 1
Cu^+ affinities of reference amino acids (kJ mol^{-1})

Amino acid (B_i)	$\Delta H^\circ_{Cu^+}(B_i)$[a]
Alanine (Ala)	275.7
Serine (Ser)	282.0
Leucine (Leu)	286.2
Isoleucine (Ile)	287.0
Glutamine (Gln)	307.6
Tryptophan (Trp)	316.7
Histidine (His)	324.7

[a]Obtained by anchoring the relative Cu^+ affinities of the amino acids in respect to glycine, as determined by the kinetic method [11], to the absolute Cu^+ affinity of Gly (at 298 K) obtained by ab initio theory [12].

required for their use as B_i by the kinetic method variant applied here (vice supra).

4.1. Angle-resolved CAD mass spectra of methanol and n-butylbenzene ions

In ARMS, the CAD fragments from a kiloelectron volt precursor ion are monitored at various scattering angles [18–20]. A larger (smaller) scattering angle corresponds to precursors that were deposited a higher (lower) average internal energy on collision. The scattering angle can be defined *after* the collision by employing a moveable slit to detect fragment ions at a selected direction, or *before* the collision by deflecting the precursor ion. Cooks et al. have reported that the latter process is preferable because it allows for rapid access to any desired angle and shows superior sensitivity and angular resolution [19]. Our instrumental setup permits precollision deflection of an ion beam in the x–y plane [31]. Acquiring the CAD spectra of $CH_3OH^{+\cdot}$ as a function of the deflection potential (and, hence, the deflection angle) and plotting the normalized fragment ion abundances versus the deflection potential leads to the breakdown graph of Fig. 1(a). This graph is in excellent agreement with the ARMS spectrum of $CH_3OH^{+\cdot}$ obtained by Cooks et al. [19], cf. Fig. 1(b), pointing out that our instrumentation provides adequate angular resolution for the selection of a given scattering angle, corresponding to a given precursor ion internal energy. To further verify our capability to sample ions of different internal energies, the collision-induced fragmentation of ionized n-butylbenzene to $C_7H_7^+$ and $C_7H_8^+$ was measured at various scattering angles to create the breakdown curve of Fig. 2(a); for comparison, Fig. 2(b) depicts relevant PEPICO data by Baer *et al.* [34]. The similarity of Fig. 2(a) and (b) once more indicates that precollision deflection of the ion beam in the x–y plane allows us to sample precursor ions with different internal energies.

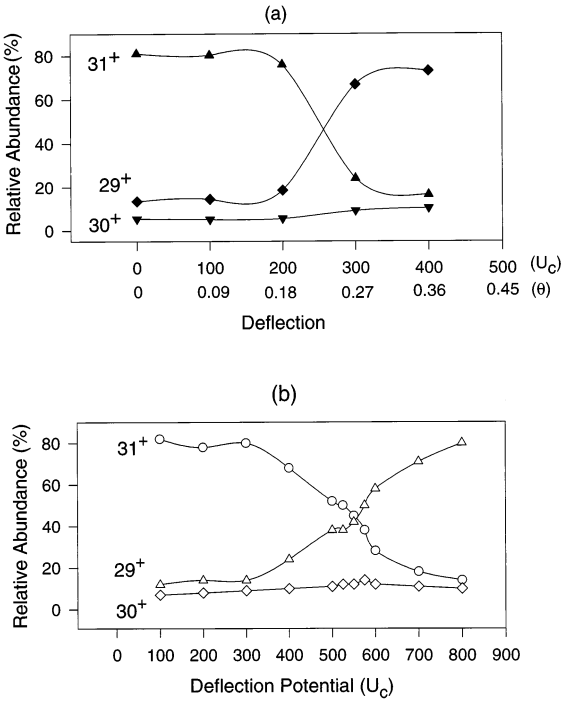

Fig. 1. Angle-resolved CAD mass spectra of methanol ion obtained by precollision deflection of the $CH_3OH^{+\cdot}$ main beam, plotted in breakdown curve form. (a) Present work; (b) adapted from [19] with permission from Elsevier Science.

4.2. Tandem mass spectra of Cu^+-bound heterodimers

The MI spectra of dimer ions $[A + B_i]Cu^+$ essentially show two products, viz. the $[A]Cu^+$ and $[B_i]Cu^+$ fragments generated according to Eq. (3). This is illustrated for $[Val + Ile]Cu^+$ in Fig. 3(a). The metastable $[A]Cu^+$ and $[B_i]Cu^+$ peaks have Gaussian shape and their peak widths at half height correspond

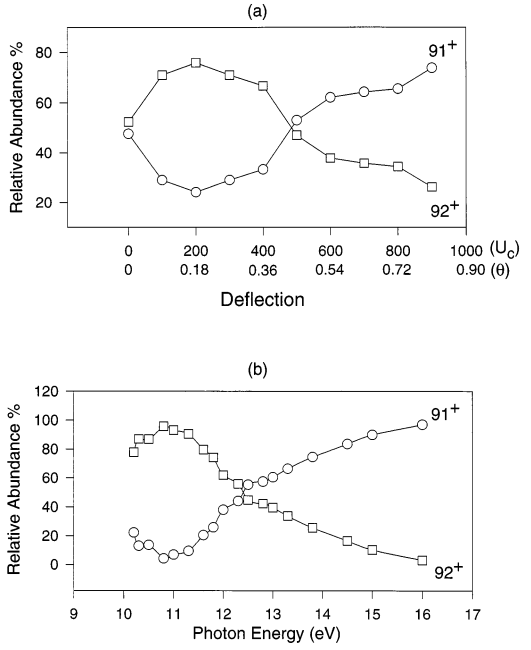

Fig. 2. (a) Angle-resolved CAD spectra of n-butylbenzene ion obtained in the present study by precollision deflection of the $C_{10}H_{14}^{+\cdot}$ main beam, plotted in breakdown curve form (*m/z* 91–92). (b) Breakdown curve of n-butylbenzene ion to *m/z* 91 and 92, adapted from Ref. 34 with permission from the American Chemical Society.

to kinetic energy releases of ≤20 meV. These characteristics confirm that the competitive dissociations of Eq. (3) proceed endothermically without appreciable reverse activation energy [32,33], as assumed by the experimental method used.

The competitive eliminations of A and B_i remain as the principal decomposition channels also after collisional activation, as revealed in Fig. 3(b) by the CAD spectrum of [Val + Ile]Cu^+. CAD causes some consecutive fragmentation of [A]Cu^+ and [B_i]Cu^+ (mainly by CH_2O_2 loss [6–9]), but no interligand fragments (containing pieces of A *and* B_i) are detected, substantiating that the two amino acids forming the dimer are bridged via a central Cu^+ ion, viz. A–Cu^+–B_i; such a connectivity is a prerequisite for using the kinetic method to determine bond energies.

For all dimers studied, the degree of consecutive fragmentation stays low at the target pressures and deflection angles used in the ARMS experiments (about ≤10%) and is much less sensitive to variations in the deflection angle than the intensity ratio of the primary dissociation products [A]Cu^+ and [B_i]Cu^+. If the abundances of the consecutive fragments are added to those of [A]Cu^+ and [B_i]Cu^+, the apparent Cu^+ basicities do not change appreciably (±<0.2 kJ mol^{-1}). The quality of the regression lines of Eq. (6) worsens, however, with the sequential fragments added, possibly because of the error introduced by the extra data manipulation. For this reason, only the [A]Cu^+ and [B_i]Cu^+ ions have been considered for the derivation of apparent basicities. The effect of consecutive fragmentation is found to be similarly negligible when different target gases (instead of ARMS are used to vary T_{eff} [24,25].

4.3. Cu^+ affinities via the dissociation of Cu^+-bound dimers at different internal energies

The experimental procedure is exemplified in detail for valine. The dissociations of [Val + B_i]Cu^+ (B_i = Ala, Ser, Leu, Ile) were assessed at four effective temperatures, corresponding to collisionally activated decompositions observed at 0, 100, 200, and 300 V of deflecting potential, or 0.00, 0.09, 0.18, and 0.27 degrees of deflection. Plotting $\ln(k/k_i)$, i.e. the monomer abundance ratios, from these dissociations versus $\Delta H^\circ_{Cu^+}(B_i)$ affords the four regression lines included in Fig. 4. According to Eq. (6), the slopes of these lines yield the effective temperatures of the [Val + B_i]Cu^+ dimers sampled at the selected θ, viz. $T_{eff/\theta}$, and the intercepts yield the respective apparent copper(I) ion basicities of Val at these $T_{eff/\theta}$, viz. $\Delta G^{app}_{Cu^+}(Val)_\theta$, which are summarized in Table 2. With these data, a plot of $\Delta G^{app}_{Cu^+}(Val)_\theta/RT_{eff/\theta}$ versus $1/RT_{eff/\theta}$ can be generated, cf. Eq. (7) and Fig. 5, to provide the copper(I) ion affinity of Val, viz. $\Delta H^\circ_{Cu^+}(Val)$, from the slope and the relative entropy of the Val–Cu^+ and B_i–Cu^+ bonds, viz. $\Delta(\Delta S^\circ_{Cu^+})$, from the intercept; their actual values are included in Table 2. The same experimental procedure was followed to derive the copper(I) ion affinities of lysine and arginine from the collision-induced fragmentations of [Lys + B_i]Cu^+ (B_i = Phe, Trp, His) and [Arg + B_i]Cu^+ (B_i = Gln, His) at four different

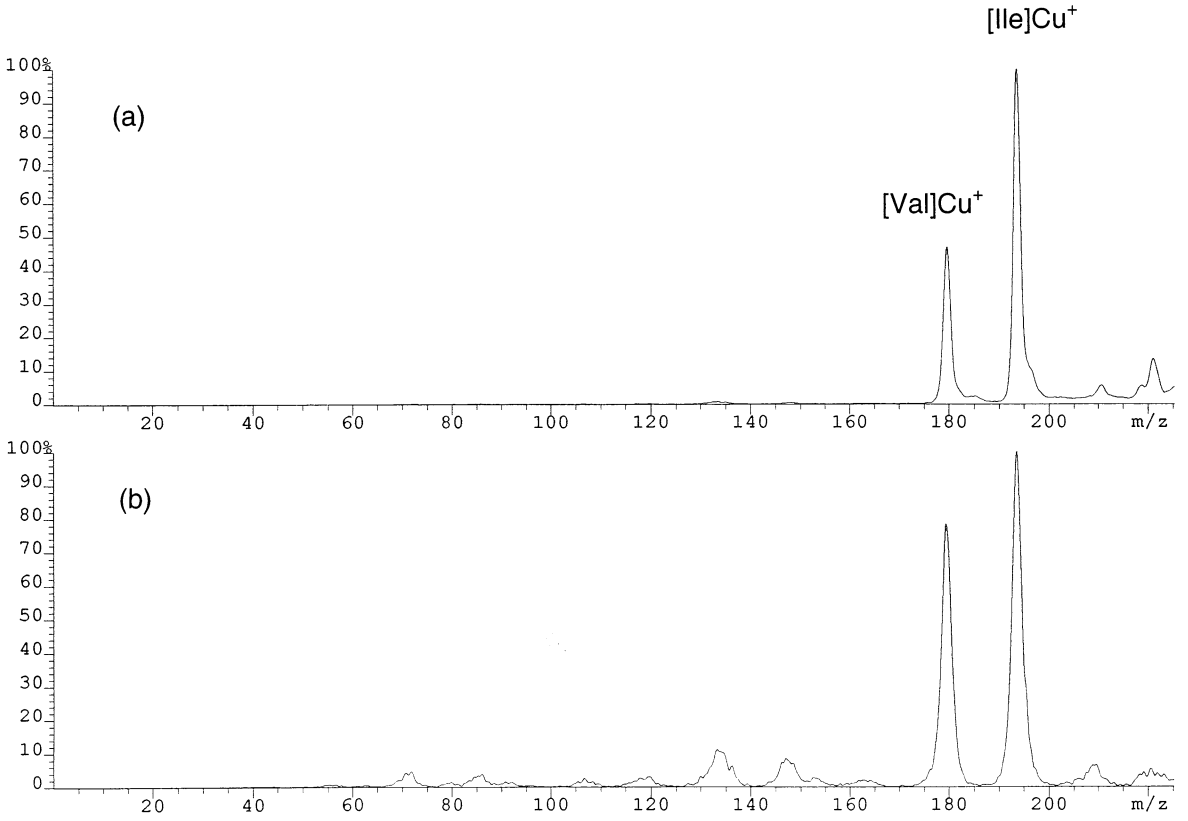

Fig. 3. (a) MI and (b) CAD/He spectra of heterodimer [Val + Ile]Cu^+.

scattering angles. Table 2 lists the corresponding $T_{\mathrm{eff}/\theta}$ and $\Delta G^{\mathrm{app}}{}_{\mathrm{Cu}^+}$ values, as well as the Cu^+ affinities and relative entropies resulting from them when $\Delta G^{\mathrm{app}}{}_{\mathrm{Cu}^+}/RT_{\mathrm{eff}/\theta}$ is plotted versus $1/RT_{\mathrm{eff}/\theta}$. The latter plots are illustrated in Fig. 5; the excellent linear correlations in this type of regression lines attests that $\Delta(\Delta S^{\circ}{}_{\mathrm{Cu}^+}) = \Delta S^{\circ}{}_{\mathrm{Cu}^+}(\mathrm{A}) - \Delta S^{\circ}{}_{\mathrm{Cu}^+}(\mathrm{B}_i)$ remains constant with the amino acids used for B_i (Table 1), in keeping with our previous study that found similar entropies of Cu^+ complexation for all common α-amino acids excluding Lys and Arg. This fact is further supported by the negligible relative entropy obtained here for valine (Table 1). As a consequence, the Cu^+ affinity of valine acquired by the combined kinetic/ARMS method (283 kJ mol^{-1}, Table 1) closely resembles the value established earlier (284 kJ mol^{-1} [11,12]) by the simple kinetic method under the assumption that $\Delta(\Delta S^{\circ}{}_{\mathrm{Cu}^+}) \approx 0$ for Cu^+-bound dimers not containing Lys or Arg.

The copper(I) ion affinities of lysine and arginine (355 and 364 kJ mol^{-1}, respectively) are found to be considerably larger than that of histidine (325 kJ mol^{-1}). Apparently, the strongly basic *and* flexible side chains of Lys and Arg enable them to fold and align their functional groups better than any other amino acids with functionalized side chains, so that Cu^+ is coordinated very efficiently in stable pseudocyclic structures without significant strain. At this point it is noteworthy that lysine and arginine also have markedly higher proton affinities (996 and 1051 kJ mol^{-1}, respectively [35]) in comparison to histidine (988 kJ mol^{-1} [35]). The increased proton affinities of Lys and Arg are partly because of the strong intramolecular solvation (hydrogen bonding)

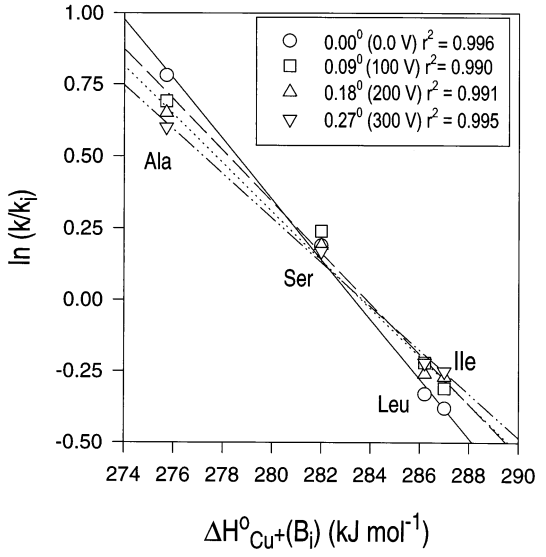

Fig. 4. Plot of $\ln(k/k_i)$ vs. $\Delta H^\circ_{Cu^+}(B_i)$ at four effective temperatures for heterodimers $[Val + B_i]Cu^+$ (B_i = Ala, Ser, Leu, and Ile), cf. Eq. (6). The rate constant ratio k/k_i is equal to the ratio of the abundances of $[Val]Cu^+$ and $[B_i]Cu^+$ observed at the respective deflection potential (scattering angle).

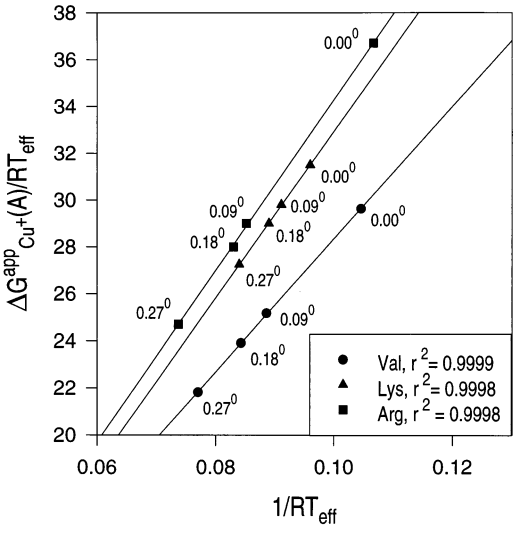

Fig. 5. Plot of $\Delta G^{app}_{Cu^+}(A)_\theta/RT_{eff/\theta}$ vs. $1/RT_{eff/\theta}$ for heterodimers $[A + B_i]Cu^+$, cf. Eq. (7). This plot is equivalent to a plot of the intercepts vs. negative slopes of the regression lines generated by Eq. (6). ● $[Val + B_i]Cu^+$ (B_i = Ala, Ser, Leu, and Ile). ▲ $[Lys + B_i]Cu^+$ (B_i = Phe, Trp, and His). ■ $[Arg + B_i]Cu^+$ (B_i = Gln and His).

of the added proton, made possible by the long, flexible side chains of these amino acids [22, 35, 36]. The high Cu^+ affinities of lysine and arginine could similarly originate from their flexible side chains enabling intramolecular multidentate coordination with particularly stable geometries in the corresponding copper(I) complexes. Scheme 2 displays plausible structures that could account for the increased Cu^+ affinity of Lys and Arg [37, 38].

The relative entropy of Cu^+ complexation, viz. $\Delta(\Delta S^\circ_{Cu^+})$, is significant for Lys (+ 22 J mol^{-1} K^{-1}) and Arg (+18 J mol^{-1} K^{-1}). This means that Cu^+

Table 2
Cu^+ affinities and relative entropies of Cu^+ attachment of the amino acids (A) Val, Lys, and Arg, deduced from the dissociation of $[A + B_i]Cu^+$ dimers (B_i = Ala, Ser, Leu, Ile, Trp, Gln, and His)[a]

	Val	Lys	Arg
$\theta = 0.00°$			
T_{eff} (K)	1150	1253	1127
$\Delta G^{app}_{Cu^+}$ (kJ mol^{-1})	283.2	328.1	344.0
$\theta = 0.09°$			
T_{eff} (K)	1358	1320	1412
$\Delta G^{app}_{Cu^+}$ (kJ mol^{-1})	284.0	327.1	340.4
$\theta = 0.18°$			
T_{eff} (K)	1427	1351	1450
$\Delta G^{app}_{Cu^+}$ (kJ mol^{-1})	283.6	325.1	337.2
$\theta = 0.27°$			
T_{eff} (K)	1562	1432	1632
$\Delta G^{app}_{Cu^+}$ (kJ mol^{-1})	283.4	324.4	335.1
$\Delta(\Delta S^\circ_{Cu^+})$ (J mol^{-1} K^{-1})	−0.6	+22.0	+18.0
$\Delta H^\circ_{Cu^+}$ (kJ mol^{-1})	283	355	364

[a]The error limits are ±70 K for T_{eff}, ±3 J mol^{-1} K^{-1} for $\Delta(\Delta S^\circ Cu^+)$ and ±5 kJ mol^{-1} for $\Delta H^\circ_{Cu^+}$.

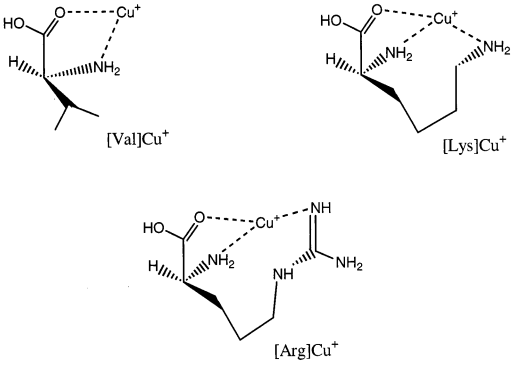

Scheme 2.

attachment to either of these amino acids (A) brings upon markedly larger entropy changes than Cu^+ attachment to the reference amino acids Phe, Gln, Trp, and His (B_i). Note that Lys and Arg carry much longer side chains than B_i. As a result, participation of the side chain substituent in the coordination of Cu^+ in pseudocyclic conformations would restrict a much larger number of rotations (or torsions) in Lys and Arg than in B_i (cf. Scheme 2), justifying the higher values of $\Delta S^\circ_{Cu^+}$(Lys) and $\Delta S^\circ_{Cu^+}$(Arg) vis à vis $\Delta S^\circ_{Cu^+}(B_i)$. Again, it is worth mentioning that Lys and Arg have the largest entropies of protonation among the common α-amino acids, caused by the folding of their protonated forms through strong intramolecular hydrogen bonding ($\Delta S^\circ_{H^+}$ in joules per mole kelvin is 151 for Lys, 149 for Arg and 114–127 for the other α-amino acids [35]). Our results (Table 2) point out that Cu^+ complexation and protonation of Lys or Arg induce "folding" interactions of comparable magnitude.

5. Conclusions

The kinetic method has been combined with angle-resolved mass spectrometry to assess the Cu^+ binding to valine, lysine, and arginine by measuring the competitive dissociations of Cu^+-bound heterodimers between these and other α-amino acids as a function of effective temperature. This approach allows one to derive both Cu^+ affinities and relative entropies of Cu^+ complexation from experimentally measured apparent free energies. Lys and Arg are found to have the largest Cu^+ affinities and entropies of Cu^+ complexation among the 20 mammalian amino acids. The combined affinity and entropy data are consistent with multidentate binding of Cu^+ by Lys and Arg in which their long, flexible side chains fold to provide a particularly stable coordination arrangement to the metal ion.

Angle-resolved CAD mass spectrometry can be used to vary the internal energy and, hence, the effective temperature of kiloelectron volt dimer ions continuously and in small steps (similar to energy-resolved CAD in the electron volt domain). The apparent free energies of Cu^+ complexation are generally found to follow an excellent linear correlation with the corresponding effective temperatures (Fig. 5). Obtaining only 2–3 data points (as done in our earlier studies [23–25]) does, therefore, not appear to compromise the quality (error limit) of the deduced affinity and entropy values.

Acknowledgements

The authors thank the National Institutes of Health, the University of Akron, and the Ohio Board of regents for their financial support and Dr. Michael J. Polce for stimulating discussions.

References

[1] S.J. Lippard, J.M. Berg, Principles of Bioinorganic Chemistry, University Science Books, Mill Valley, CA, 1994, and references therein.
[2] W. Kaim, B. Schwederski, Bioinorganic Chemistry: Inorganic Elements in the Chemistry of Life, Wiley, Chichester, 1994.
[3] J.A. Cowan, Inorganic Biochemistry: An Introduction, 2nd ed., Wiley–VCH, New York, 1996, and references therein.
[4] R.P. Grese, R.L. Cerny, M.L. Gross, J. Am. Chem. Soc. 111 (1989) 2835.
[5] R.W. Nelson, T.W. Hutchens, Rapid Commun. Mass Spectrom. 6 (1992) 4.
[6] S. Bouchonnet, Y. Hoppilliard, G. Ohanessian, J. Mass Spectrom. 30 (1995) 172.
[7] D. Wen, T. Yalcin, A.G. Harrison, Rapid Commun. Mass Spectrom. 9 (1995) 1155.
[8] Q.P. Lei, I.J. Amster, J. Am. Soc. Mass Spectrom. 7 (1996) 722.
[9] M.J. Polce, Š. Beranová, M.J. Nold, C. Wesdemiotis, J. Mass Spectrom. 31 (1996) 1073.
[10] H. Lavanant and Y. Hoppilliard, J. Mass Spectrom. 32 (1997) 1037.
[11] B.A. Cerda, C. Wesdemiotis, J. Am. Chem. Soc. 117 (1995) 9734.
[12] S. Hoyau, G. Ohanessian, J. Am. Chem. Soc. 119 (1997) 2016.
[13] A. Luna, B. Amekraz, J. Tortajada, Chem. Phys. Lett. 266 (1997) 31.
[14] A. Luna, B. Amekraz, J.P. Morizur, J. Tortajada, J. Phys. Chem. 101 (1997) 5931.
[15] H. Deng, P. Kebarle, J. Am. Chem. Soc. 120 (1998) 2925.
[16] S.A. McLuckey, D. Cameron, R.G. Cooks, J. Am. Chem. Soc. 103 (1981) 1313.
[17] R.G. Cooks, J.S. Patrick, T. Kotiaho, S.A. McLuckey, Mass Spectrom. Rev. 13 (1994) 287.

[18] J.A. Laramee, P.H. Hemberger, R.G. Cooks, J. Am. Chem. Soc. 101 (1979) 6460.
[19] S. Verma, J.D. Ciupek, R.G. Cooks, A.S. Schoen, P. Dobberstein, Int. J. Mass Spectrom. Ion Processes 52 (1983) 311.
[20] J.J. Zwinselman, S. Nacson, A.G. Harrison, Int. J. Mass Spectrom. Ion Processes 67 (1985) 93.
[21] X. Cheng, Z. Wu, C. Fenselau, J. Am. Chem. Soc. 115 (1993) 4844.
[22] Z. Wu, C. Fenselau, Rapid. Commun. Mass Spectrom. 8 (1994) 777.
[23] B.A. Cerda, C. Wesdemiotis, J. Am. Chem. Soc. 118 (1996) 11184.
[24] B.A. Cerda, S. Hoyau, G. Ohanessian, C. Wesdemiotis, J. Am. Chem. Soc. 120 (1998) 2437.
[25] M.J. Nold, B.A. Cerda, C. Wesdemiotis, J. Am. Soc. Mass Spectrom., in press.
[26] K.J. Laidler, Chemical Kinetics, 3rd ed., Harper and Row, Cambridge, 1987, p. 112.
[27] See, for example: P.B. Armentrout, B.L. Kickel, in B.S. Freiser (Ed.), Organometallic Ion Chemistry, Kluwer Academic, Dordrecht, 1996, p. 1.
[28] K. Vekey, J. Mass Spectrom. 31 (1996) 445.
[29] S.L. Craig, M. Zhong, J.I. Brauman, J. Phys. Chem. 101 (1997) 19.
[30] K.L. Busch, G.L. Glish, S.A. McLuckey, Mass Spectrometry/Mass Spectrometry, VCH Publishers, New York, 1988.
[31] M.J. Polce, M.M. Cordero, C. Wesdemiotis, P.A. Bott, Int. J. Mass Spectrom. Ion Processes 113 (1992) 35.
[32] R.G. Cooks, J.H. Beynon, R.D. Caprioli, G.R. Lester, Metastable Ions, Elsevier, Amsterdam, 1973.
[33] J.L. Holmes, Org. Mass Spectrom. 20 (1985) 169.
[34] T. Baer, O. Dutuit, H. Mestdagh, C. Rolando, J. Phys. Chem. 92 (1988) 5674.
[35] E.P Hunter, S.G. Lias, in W.G. Mallard, P.J. Linstrom (Eds.), NIST Chemistry WebBook, NIST Standard Reference Database Number 69, National Institute of Standards and Technology, Gaithersburg, MD 20899, March 1998 (http://webbook.nist.gov).
[36] A.A. Bliznyuk, H.H. Schaefer III, I.J. Amster, J. Am. Chem. Soc. 115 (1993) 5149.
[37] C.W. Bauschlicher Jr., S.R. Langhoff, H. Partridge, J. Chem. Phys. 94 (1991) 2068.
[38] S.R. Langhoff, C.W. Bauschlicher, Jr., H. Partridge, M. Sodupe, J. Phys. Chem. 95 (1991) 10677.